# *Climate variability alters flood timing across Africa*

Geophysical Research Letters

RESEARCH LETTER
10.1029/2019GL081988

# Climate Variability Alters Flood Timing Across Africa

**Andrea Ficchì**[1] **and Liz Stephens**[1]

[1]Department of Geography and Environmental Science, University of Reading, Whiteknights, UK

**Key Points:**
- Modes of climate variability in the Pacific and Indian Oceans drive significant changes in flood timing across sub-Saharan Africa
- The hydrological system enhances and alters climate variability signals seen in rainy season onset, duration, and total rainfall
- Understanding of how climate variability changes the timing of floods can support flood-based farming systems

**Supporting Information:**
- Supporting Information S1

**Correspondence to:**
A. Ficchì,
a.ficchi@reading.ac.uk

**Citation:**
Ficchì, A., & Stephens, L. (2019). Climate variability alters flood timing across Africa. *Geophysical Research Letters*, *46*, 8809–8819. https://doi.org/10.1029/2019GL081988

Received 9 JAN 2019
Accepted 20 JUN 2019
Accepted article online 1 JUL 2019
Published online 5 AUG 2019



**Abstract** Modes of climate variability are known to influence rainy season onset, but there is less understanding of how they impact flood timing. We use streamflow reanalysis and gauged observation data sets to examine the influence of the Indian Ocean Dipole and El Niño–Southern Oscillation across sub-Saharan Africa. We find significant changes in flood timing between positive and negative phases of both Indian Ocean Dipole and El Niño–Southern Oscillation; in some cases the difference in the timing of annual flood events is more than three months. Sensitivity to one or other mode of variability differs regionally. Changes in flood timing are larger than variability in rainy season onset reported in the literature, highlighting the need to understand how the hydrological system alters climate variability signals seen in rainy season onset, length, and rainfall totals. Our insights into flood timing could support communities who rely on flood-based farming systems to adapt to climate variability.

**Plain Language Summary** Patterns of climate variability such as the El Niño–Southern Oscillation or the Indian Ocean Dipole affect the timing of the start of the rainy season, but little is known about how this translates into changes in the timing of the annual flood in rivers. We use computer model reconstructions and observed records of river flows in Africa to understand how these patterns of climate variability are changing the timing of river floods. In eastern and southern Africa, in particular, the differences in flood timing can be more than three months. This information could help farmers in African floodplains to adapt their water management, planting, and cropping practices to these patterns of climate variability.

## 1. Introduction

Teleconnections to major climate modes, such as the El Niño–Southern Oscillation (ENSO) or the Indian Ocean Dipole (IOD), strongly influence seasonal rainfall anomalies and rainy season timing in large parts of Africa (e.g., Behera et al., 2005; Dunning et al., 2016; Marchant et al., 2007; Nicholson, 2000), in turn affecting the interannual variability in river flows. The climatological regimes, timing, and duration of the rainy seasons are different across regions of Africa (Dunning et al., 2016; Herrmann & Mohr, 2011). Climate modes evolve differently depending on the season and also rainfall teleconnections vary regionally and seasonally (Rowell, 2013); for example, IOD impacts eastern Africa during October–December. However, the relationship of flood hazard to rainfall anomalies is strongly nonlinear (Coughlan de Perez et al., 2017; Stephens et al., 2015), so it is important to analyze the relationship between river flows and climate variability directly and over different spatiotemporal scales. While there are several studies about the impact of teleconnections (especially ENSO) on flood likelihood and magnitude at global and regional scales (e.g., Chiew & McMahon, 2002; Emerton et al., 2017; Ward et al., 2014), their impact on flood timing has been addressed by only a few studies beyond the catchment scale (e.g., Sharif & Burn, 2009; Stewart et al., 2005).

Understanding how climate variability affects flood timing has applications for water resources planning and management (Cunderlik & Ouarda, 2009). Changes in the timing of the annual flood, for example, have widespread impacts on flood-based farming systems and therefore the livelihoods for populations who adapt their floodplain management and agricultural practices to the normally experienced rise and fall of the flood wave (Paul, 1984; van Steenbergen, 1997). Accordingly, research has been carried out to characterize the distribution of hydrological regimes globally (Dettinger & Diaz, 2000; Lee et al., 2015), to explain the largest seasonality gradients (Hastenrath, 1996), and to understand how hydrological regimes might be impacted by climate change (Blöschl et al., 2017; Burn et al., 2016; Cunderlik & Ouarda, 2009).

The objective of this paper is to investigate whether there are significant differences in the timing of annual floods between different modes of climate variability across Africa, where there is a strong link between

climate modes and seasonal regional rainfall, and where flood-based farming systems are used extensively (Mehari et al., 2011; Scudder, 1991). In this study, we consider only ENSO and IOD, as two prominent modes of climate variability, while we acknowledge that other modes originating in the Atlantic or Indian Ocean also influence rainfall in different parts of Africa. We first characterize continental-scale seasonality in flooding to define a baseline for annual maximum flow timing and then compare the timing of the annual flood during different ENSO/IOD events. We use a reanalysis data set to provide continental-scale coverage, but compare this to results obtained from a stream-gauge data set. Finally, we show how a better understanding of the timing of floods could be used to improve the resilience of vulnerable farming communities in floodplains.

## 2. Data and Methods

### 2.1. Streamflow Data Sets

The river flow data used in this study include the following:

1. A global daily reanalysis at 0.1° resolution for the 36-year period 1980–2015, derived by forcing a global-scale hydrological model, GloFAS, the Global Flood Awareness System (Alfieri et al., 2013), with the ERA-Interim/Land meteorological reanalysis (with horizontal resolution of about 80 km and 3-hourly time step) produced using the revised land surface hydrology version of the Tiled ECMWF Scheme for Surface Exchanges and incorporating the Global Precipitation Climatology Project-based bias corrections (Balsamo et al., 2009; Balsamo et al., 2015). The LISFLOOD hydrological model (Van Der Knijff et al., 2010) is used for flow routing in GloFAS. We selected 18,118 river cells in sub-Saharan Africa (SSA; study area: −17.75 to 51.25 longitude, −34.75 to 16.05 latitude) with an upstream area >5,000 $km^2$.
2. Sixty-five SSA stream-gauge daily observations from the Global Runoff Data Centre data set (BfG, 2017). The selected records were chosen to ensure an adequate sample size and have (1) ≥18 years of daily observations available within the 36-year study period 1980–2015, with gaps of <5% for each year; (2) at least five hydrological years per phase of ENSO/IOD (see section 2.2); and (3) no gap-filling artifacts or evidence of water management.

The streamflow reanalysis is considered suitable for this study, given that atmospheric variables from ERA-Interim compared well with respect to other products over the study region (e.g., Moalafhi et al., 2016) and the river discharge produced with ERA-Interim/Land showed a good correlation with observations across Africa (see Balsamo et al., 2015, Figure 7). We do not use the calibrated version of the GloFAS model (Hirpa et al., 2018), which means the stream-gauge observations can be used as an independent benchmark. Since the GloFAS model accounts only for a relatively few reservoirs and dams in Africa (Zajac et al., 2017) and does not take account of other human regulation, the reanalysis is representative of near-natural river flows. Ideally, the comparison between the two products should take human regulation into account, but there are only two pristine river basins (defined by Global Runoff Data Centre to have no significant regulation and minimal development) in the stream-gauge data set, the Cubango-Okavango River at Rundu (Namibia) and the Nyando River at Ahero (Kenya), and only the first meets the data requirements. Unfortunately, the observational data set underrepresents some large flood-prone regions across SSA (e.g., Mozambique, Malawi, and Madagascar), for which we rely on the reanalysis.

### 2.2. Choice and Definition of Climate Modes

The ENSO is often considered as the primary driver of seasonal rainfall variability over the African continent (Nicholson, 2017; Nicholson & Kim, 1997), although several studies have pointed to the importance of other climate modes, including the IOD (Saji et al., 1999) for rainfall anomalies mainly in eastern Africa (Behera et al., 2005; Black, 2005; Marchant et al., 2007; Saji & Yamagata, 2003). In this study, we look at the impact of both ENSO and IOD on flood timing. Other climate modes influence rainfall anomalies across large parts of Africa such as the Subtropical Indian Ocean Dipole (Behera & Yamagata, 2001), the Benguela Niño, and other Atlantic sea surface temperature (SST) modes (Camberlin et al., 2001; Nicholson & Entekhabi, 1987; Rouault et al., 2003; Todd & Washington, 2004). These modes were not considered in this study mainly because of the large differences in their seasonality with respect to ENSO/IOD; for example, Benguela Niños tend to occur in February–April (Reason & Smart, 2015), and Subtropical Indian Ocean Dipole usually peak in February (Behera & Yamagata, 2001), which would require a wider analysis framework

for seasonality than the one chosen here using a common hydrological year definition (since both ENSO/IOD occur later in the calendar year; see Figure S2).

We use a quantile-based (tercile) threshold approach to categorize negative (bottom 33%), neutral (middle 33%) and positive (upper 33%) values of the index associated with each mode of climate variability. Each of the terciles is therefore represented by 12 years of data. El Niño/La Niña events are identified based on the three-month running mean of the monthly global analysis Extended Reconstructed Sea Surface Temperature version 5 (Huang et al., 2017) anomalies for the Niño-3.4 region (170°W to 120°W, 5°N to 5°S). An El Niño/La Niña year is defined when a positive/negative peak of SST during August to December is in the top/bottom 33% of the monthly SST anomalies of the whole 36-year data set. The IOD positive and negative phases (IOD+/−) are identified based on the Dipole Mode Index (Saji et al., 1999) which is the difference between SST anomalies in the western (50°E to 70°E and 10°S to 10°N) and eastern (90°E to 110°E and 10°S to 0°S) equatorial Indian Ocean. We used monthly Dipole Mode Index data (www.esrl.noaa.gov/psd/gcos_wgsp/Timeseries/DMI/, derived from HadISST data set). Positive/negative phases of the IOD are defined as the years when the peak of the Dipole Mode Index over June to November is in the top/bottom 33% over the 36-year period. Similarities in the impacts of ENSO and IOD on river flows might be expected because ENSO/IOD events, especially positive phases, tend to co-occur (Wolff et al., 2011). However, there is still some independence between the two climate modes: within our time series there are 8 out of 12 concurrences of ENSO+ and IOD+ and 3 out of 12 concurrences of ENSO− and IOD− (Figures S1a and S1b).

### 2.3. Streamflow Peak Seasonality

We extracted annual maximum flow over a hydrological year starting from September through to the following August. This ensures we only consider river flows which follow the ENSO and IOD (+/−) event development phase (Figure S2). To avoid double-counting of flood events extending over the end of the hydrological year, we leave a period of at least one month from the previous annual maximum flow. We use origin-invariant metrics to describe the seasonality of annual maximum flow limiting the influence of the choice of the starting month of the hydrological year on the results.

We use directional statistics (Mardia, 1972) to calculate a seasonality index, the Burn's vector (Burn, 1997). The components represent the average timing (i.e., mean date of occurrence, $\theta$ ) and its variability ($r$), as polar coordinates on a unit circle (see Burn, 1997, equations (1)–(5)). The average flood timing, $\theta$ [rad], is calculated as the circular mean of all annual maximum flow dates converted to angular values. The variability of flood timing, $r$ [−], ranges from $r = 0$, when flood events are distributed evenly throughout the year (highly variable regimes), to $r = 1$, when they occur at the same time every year. Thus, high values of $r$ are associated with unimodal regimes with low interannual variability, while lower values, with high interannual variability, are associated with bimodal or multimodal regimes, regimes where the flow is constant or low, or where climate modes change the timing from one year to the next. To analyze the correlation between the Burn's vector angular values ($\theta$) of flood date in observations and reanalysis, we use a circular (origin-invariant) version of the Pearson correlation coefficient (Jammalamadaka & SenGupta, 2001).

To characterize the change in the timing of annual maximum flow, we calculate the difference in days between the flood timing for the positive and negative phases of ENSO/IOD. We test for the significance of these differences based on nonparametric bootstrapping (see Text S1 in the supporting information).

## 3. Results

The 36-year climatology of the streamflow reanalysis data shows that there is strong spatial coherence in flood timing across regions (Figure 1a), with the annual flood occurring mainly in August through October in northern sub-Saharan Africa (including the Sahel and Guinea region), April–June in the Horn of Africa (except the Shabelle River and Ethiopian Highlands), and December through March in southern Africa (except the most southwestern part). In most of these regions, the flood timing (Figure 1b) is highly predictable ($r > 0.7$), with only eastern Africa and the southwestern part of southern Africa showing $r$ values <0.63. Seasonality in flood timing largely corresponds to the movement of the Intertropical Convergence Zone southward/northward. In July/August, the Intertropical Convergence Zone lies around 18° to 20° N,

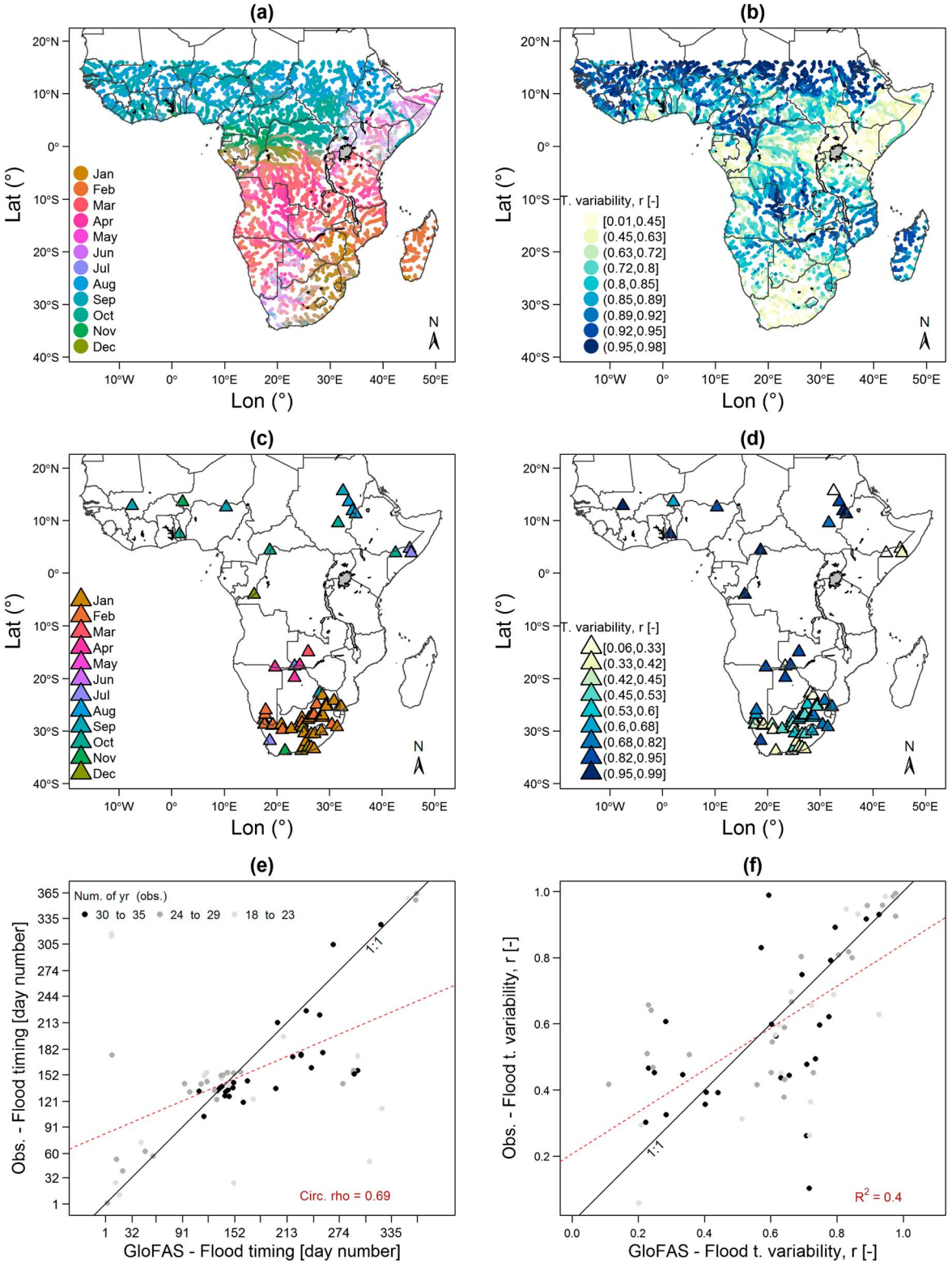


**Figure 1.** Annual flood seasonality measures for sub-Saharan Africa. (a) Average flood timing ($\theta$) based on streamflow reanalysis; the interannual variability is reported with different color saturation (the higher the variability is, the lighter the saturation is). (b) Interannual variability of flood timing ($r$ [−]) based on streamflow reanalysis. (c) Average flood timing based on stream-gauge data (triangular dots reported at gauge locations). (d) Interannual variability of flood timing based on stream-gauge data. (e) Scatterplot between mean date of flood occurrence (day number in hydrological year) in observation ($y$ axis) versus reanalysis ($x$ axis) with linear regression fit (red dashed line). (f) Scatterplot between variability of flood timing in observation versus reanalysis with linear regression fit.

with low pressure (and associated rainfall) over the Sahara and high pressure over southern Africa; from September the Intertropical Convergence Zone moves southward, reaching about 15°–18°S over south-eastern Africa in February, and bringing the wet season over central and southern Africa from November to March, before moving northward from March.

Other convergence zones, shaping circulation patterns across SSA, may explain other spatial patterns of flood timing. For example, the Congo Air Boundary location in July/August roughly corresponds to the position of the west-east abrupt shift in flood timing and variability in the Horn of Africa, alluding to the response to distinct moisture sources from the Atlantic and Indian Oceans (Nicholson, 2000). The average flood timing and variability (Figures 1a and 1b) are also consistent with the seasonality of extreme rainfall events driven by (i) cutoff lows, leading to floods in the region south of 20°S, which have high interannual variability in seasonality and frequency (Singleton & Reason, 2007); (ii) tropical cyclones, developing in the South Indian Ocean and landfalling in Madagascar and more occasionally Mozambique (with peak period from January to March; Vitart et al., 2003); (iii) monsoon depressions and the African Easterly Wave, which develop from July onward and remain over the interior of West Africa until September (Gu & Adler, 2004); and (iv) mesoscale convective complexes, associated with rainfall from central Mozambique to eastern South Africa from November to March (Blamey & Reason, 2013).

Similar patterns, both with respect to timing and predictability, emerge from analysis of the station data (Figures 1c and 1d). There is a statistically significant correlation (circular Pearson coefficient = 0.69, $p$ value $< 10^{-5}$) between average flood timing from station data and the reanalysis (Figure 1e). The strength of the correlation between interannual variability as shown by the station data and the reanalysis is poorer ($r^2$ = 0.4) but becomes stronger as r increases (Figure 1f). This suggests that the reanalysis data are less reliable in regions where the timing of flood events is very unpredictable. Nevertheless, the reasonable correlation between measures of flood timing between the two sources suggests that the reanalysis product is sufficiently reliable to obtain a spatially continuous picture of flood timing for the continent.

Flood timing sensitivity to ENSO/IOD differs regionally; differences of >60 days between negative and positive phases of ENSO/IOD are registered for 17.5% of the river network (Figures 2a and 2b). While the bootstrap test (section 2.3 and Text S1 in the supporting time) shows that there is uncertainty in the signal, there are still multiple river catchments across SSA with a significant difference between positive and negative phases of ENSO/IOD (Figures 2c and 2d). About 27% of the river cells show changes in timing between ENSO+/− phases of more than one month, and these changes are significant for 14% of all river cells. The percentages are very similar for IOD+/−: 33% of river cells have differences of more than one month and the change is significant for 16% of all cells. However, only 28% of the cells which have significant differences in flood timing between IOD+ and IOD− also show significant changes between ENSO+ and ENSO−.

The regions which show the largest differences in flood timing for both ENSO and IOD are (i) eastern Africa, mainly Kenya, Ethiopia, and Somalia (see discussion in section 4); (ii) southern Africa, mainly across the Okavango and Orange River basins (including tributaries, e.g., Vaal, and intermittent rivers in the Kalahari, e.g., Molopo); and (iii) central (equatorial) Africa, particularly a large part of the Congo River basin. Each of the regions shows different behavior with respect to the changes for ENSO and IOD, in terms of the extent of the river network affected and the magnitude of the changes. For example, a stronger signal emerges for ENSO than IOD in southern Africa (e.g., Okavango basin), while larger changes emerge for IOD in the Congo River basin (see discussion in section 4). These differences between ENSO and IOD are driven by different patterns of flood timing changes for both positive and negative phases (Figure S3), despite the higher correlation in positive ENSO/IOD phases (Figure S1). Also, an exploratory analysis based on subsampling independent and synchronous ENSO/IOD events (with at least three years per subsample) suggests a potential interference of ENSO/IOD impacts for positive phases, with a stronger signal of change in flood timing for independent ENSO/IOD events (Figure S4).

There are only a limited number of stations (Figures 2e and 2f) available for comparison with regions identified from the reanalysis (Figures 2c and 2d) as having significant changes between phases of ENSO/IOD. Furthermore, seasonal forecasts are often used to adjust reservoir management rules (e.g., Gelati et al., 2014; Oludhe et al., 2013), further reducing the likelihood of agreement between the station data and the reanalysis. Nevertheless, there is agreement between the two data sets (Figures 2a / 2b and 2e / 2f), which is generally similar across ENSO and IOD phases (Figure S5).

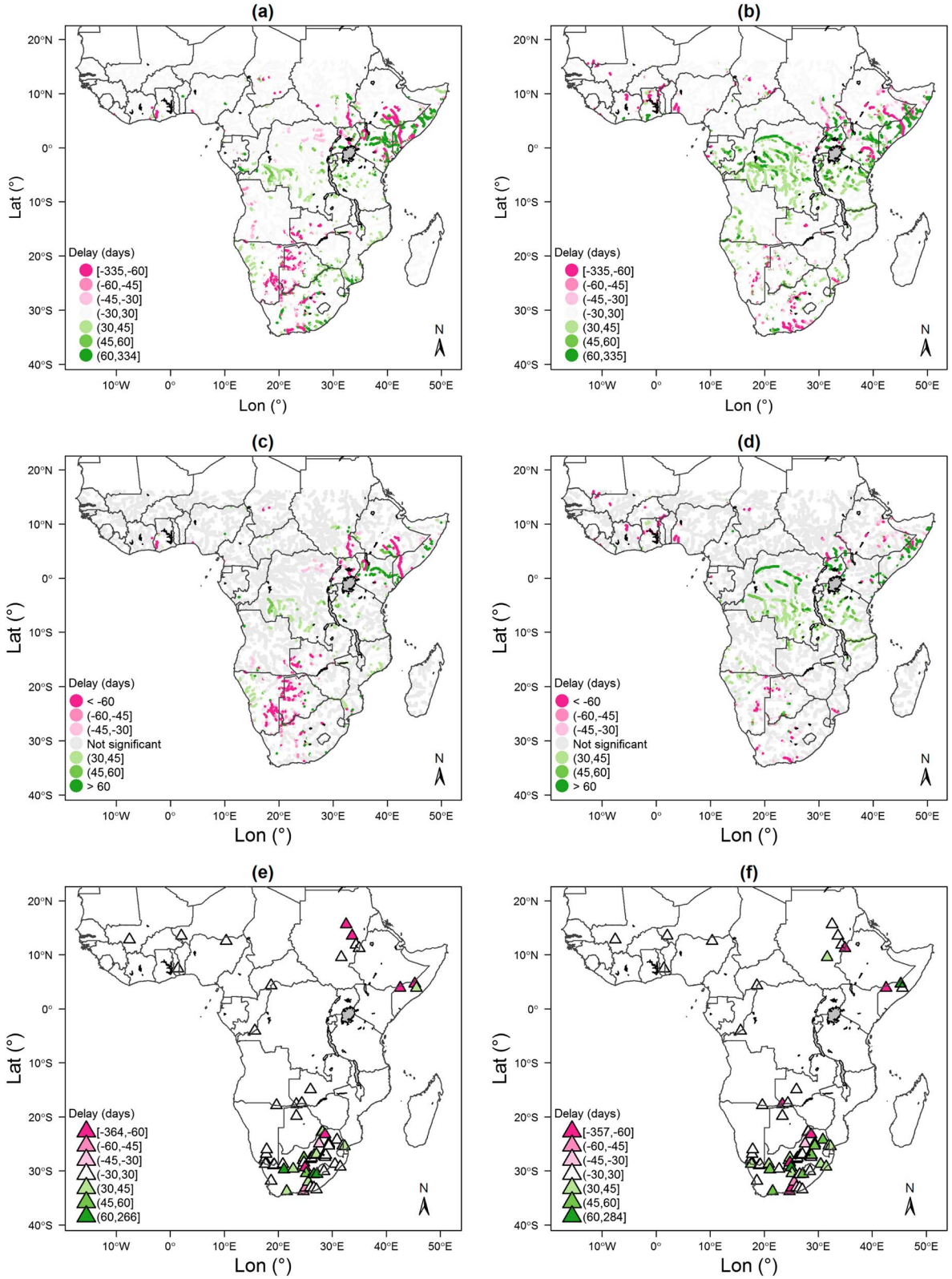


**Figure 2.** Maps of changes of annual flood timing (days) based on the streamflow reanalysis and stream-gauge data for positive and negative ENSO and IOD phases. (a, c, e) Negative ENSO with respect to positive ENSO. (b, d, f) Negative IOD with respect to positive IOD, based on GloFAS (top panels), where greyed-out cells correspond to nonsignificant changes according to nonparametric bootstrapping test on the difference of the means at 90% confidence level (middle panels), and observations (bottom), respectively. Pink (green) points correspond to river cells where floods occur earlier (later) than in the baseline (positive ENSO/IOD).

For bimodal regimes, there are two ways in which ENSO/IOD can impact annual flood timing:

1. The annual peak flood occurs in the same season across the climate modes, but with time shifts earlier or later, for example, for the Webi Jubba River in Somalia (Figure S6a). For eastern Africa, where bimodal rainfall patterns are dominant (e.g., Yang et al., 2015), we estimate this to be the most frequent case in 72% of river cells where there are significant changes in flood timing during ENSO/IOD (+/−) events (see Text S2 in the supporting information).
2. The annual flood peak shifts from one high-flow season to another, for example, for the Victoria Nile River in Uganda (Figure S6b). We estimate this to be the predominant case in 28% of river cells in eastern Africa where there are significant changes in flood timing (see Text S2 in the supporting information).

Overall, for river cells in eastern Africa which register significant changes in flood timing there is a median change of 53 days.

## 4. Discussion

The spatial signal of average flood timing and variability across large regions of Africa (Figure 1) generally corresponds to broad-scale spatial patterns of rainfall (Herrmann & Mohr, 2011; Nicholson, 2000). A few basins have distinctive flood timing and changes with ENSO/IOD which are different from the surrounding region, for example, the Jubba and Shabelle Rivers in Somalia and Ethiopia, due to influence of larger runoff contributions from upstream areas (with different seasonality) and different rainfall response to ENSO between coastal eastern Africa and Ethiopian highlands (e.g., Nicholson & Kim, 1997).

Over eastern Africa, both ENSO and IOD have a large and similar influence. This was expected given the concurrence between ENSO+ and IOD+ phases (Figure S1) and the known teleconnections between eastern African rainfall and both ENSO and IOD (Black, 2005). In central southern Africa, ENSO phases drive larger changes in flood timing than the IOD, both in terms of spatial extent of the impacts and magnitude of the signal of changes. Significant changes in flood timing with ENSO (Figure 2c) are found in the Okavango Delta and in ephemeral rivers in the Kalahari desert, where strong links between seasonal rainfall and ENSO are known, including an earlier occurrence of heavy rainfall in ENSO years (Nash & Endfield, 2008). The minor link of flood seasonality in the Congo River basin to ENSO (Figure 2a) is consistent with previous findings of a weak link with rainfall and total annual Congo River discharge (Amarasekera et al., 1997; Camberlin et al., 2001; Todd & Washington, 2004). However, there is a widespread significant impact on the timing of peak river flows in the southern section of the Congo Basin with the IOD. Nicholson and Dezfuli (2013) have also shown a significant correlation between wet periods and SSTs in the central tropical Indian Ocean for this region, although they did not look at how this affected rainfall timing.

Studies that have addressed variability in rainfall regimes across Africa have focused on onset, cessation, and duration. This limits the direct comparison with our results of the timing of the annual flood; climate variability does not necessarily lead to uniform shifts in the onset/cessation of the rainy season (Dunning et al., 2016), nor are these indicative of the distribution/amount of rainfall (Reason et al., 2005) which determine flood generation. However, across Africa there are marked differences between variability in rainy season onset/cessation and flood timing.

Across Ghana, variability in rainy season onset and duration is in the order of ±7 days (Amekudzi et al., 2015), whereas flood timing variability ranges from ±25 to ±79 days (i.e., standard deviations corresponding to $0.4 < r < 0.91$). In the Limpopo Basin, variability in rainy season onset is no more than 30 days (Tadross et al., 2005), while our results suggest flood timing variability of around ±60 days ($r = 0.59$). For equatorial East Africa, Camberlin et al. (2009) find standard deviations of 15 and 25 days for the onset of the long and short rains (respectively), and 10 and 20 days for the long and short season end, while we find variability in flood timing of around ±70 days ($r = 0.48$).

For climate variability, Dunning et al. (2016) map anomalies in rainy season onset and cessation due to El Niño using a scale extending to 14 days over Africa. In contrast, we find median changes in flood timing over eastern Africa of 53 days. These examples point to a considerable hydrological enhancement of signals in rainfall variability that needs to be better understood, using commensurate metrics. In fact, variability in rainfall onset/cessation depends on what criteria are used to define these parameters; agriculturally based definitions (e.g., Hachigonta et al., 2008) may give a too early onset, while definitions based on

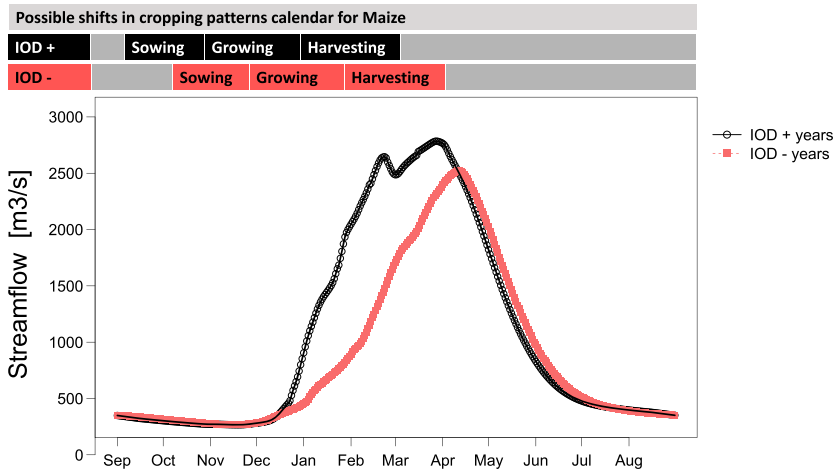


**Figure 3.** Illustration of a potential case study where the information on the expected flood timing changes could be useful for farming activities along the river plain to adapt cropping patterns (sowing, growing, and harvesting time): composite hydrograph (31-day moving average) for the Rovuma River (Mozambique) at longitude 39.65, latitude 10.95, for IOD+/− years, with hypothetical consequent cropping pattern adaptations based on a typical crop calendar (FAO/GIEWS, 2018).

cumulative anomalies potentially give a reduced season length (Dunning et al., 2016). The outcome might be different if a longer or different period of analysis was used, as suggested by MacLeod (2018), but the hydrological enhancement of rainfall signals seems robust, given the marked differences found, and the significant overlap of our study period with those of the papers mentioned above.

Further work should look at how other climate modes, such as in the Atlantic, drive flood timing, particularly over West Africa. In addition, given that climate change will alter precipitation seasonality (Dunning et al., 2018), the impact of these changes on hydrology should also be addressed. Such an analysis should consider that the catchment response might alter the changes in rainfall regimes due to potential depleted soil moisture in a warming climate (Sharma et al., 2018; Wasko & Sharma, 2017).

More than 50 million people in SSA rely on flood-based farming practices including spate irrigation, flood-recession agriculture, and cropping systems in floodplains (Mehari et al., 2011; Spate Irrigation Network, 2015; van Steenbergen, 1997). In flood irrigated areas, the crop choice is determined by the timing of the floods more than by any other preference (van Steenbergen, 1997). The timing of planting and harvesting also depends on the expected flood timing in order to make optimal use of the growing period (Phillips & McIntyre, 2000). If combined with skillful forecasts of ENSO/IOD, our results could support floodplain communities to adapt to climate variability. For example, if the annual flood is expected to occur earlier than usual, farmers could potentially shift sowing and harvesting forward to reduce the risk of flood damage and avoid harvesting immature crops (Figure 3). More accurate information on flood timing could also support flood-based fishing practices, for example, in Lake Victoria wetlands (as well as in the Sudd), which rely on flood recession timing for the creation of "fingerponds" (Kipkemboi, 2006). In regions such as the Okavango Delta, which is a tourist destination during wet periods, flood timing predictions could support planning an extended (or delayed) tourist season (Wolski & Murray-Hudson, 2006).

## 5. Conclusions

We have shown that flood timing in SSA can change significantly between positive and negative phases of ENSO and IOD. The differences in flood timing are particularly large in eastern Africa, central southern Africa, and in the Congo River basin. IOD teleconnections explain more of the flood timing variability in the Congo basin than ENSO, while ENSO explains more of the flood timing variability in central southern Africa than IOD. In eastern Africa, both ENSO and IOD have a large and similar influence. Changes in flood timing in sub-Saharan Africa are larger than variability in rainy season onset and duration reported in the literature, suggesting that the hydrological system amplifies the climate variability signals seen in

precipitation; however, further work is needed for a spatially consistent analysis of precipitation timing, using metrics commensurate with flood analysis. Further work should also consider other climate modes that influence rainfall over various parts of Africa. The improved understanding of the impact of climate variability on the timing of the annual flood could potentially be used for better management of flood-based farming systems, fisheries, and tourism across Africa and other parts of the world.

**Acknowledgments**
This work was supported by the Natural Environment Research Council and Department for International Development (grant NE/P000525/1). We thank colleagues from the FATHUM and ForPAc projects, and associated project partners (ECMWF and JRC) for the useful discussions related to this work. We thank Ervin Zsoter and Rebecca Emerton for helping with the provision of GloFAS data sets and Sandy Harrison for her comments which contributed to improving the manuscript. The streamflow reanalysis is provided through an ftp service setup by the GloFAS team upon request, by contacting the operational service at info@globalfloods.eu (see www.globalfloods.eu). The Global Runoff Data Centre (GRDC) provided the observed streamflow data set (BfG, 2017). All the analysis presented in this paper was performed in R (Core Team & R., 2017).

## References

Alfieri, L., Burek, P., Dutra, E., Krzeminski, B., Muraro, D., Thielen, J., & Pappenberger, F. (2013). GloFAS—Global ensemble streamflow forecasting and flood early warning. *Hydrology and Earth System Sciences*, *17*(3), 1161–1175. https://doi.org/10.5194/hess-17-1161-2013

Amarasekera, K. N., Lee, R. F., Williams, E. R., & Eltahir, E. A. B. (1997). ENSO and the natural variability in the flow of tropical rivers. *Journal of Hydrology*, *200*(1-4), 24–39. https://doi.org/10.1016/s0022-1694(96)03340-9

Amekudzi, L., Yamba, E., Preko, K., Asare, E., Aryee, J., Baidu, M., & Codjoe, S. (2015). Variabilities in rainfall onset, cessation and length of rainy season for the various agro-ecological zones of Ghana. *Climate*, *3*(2), 416–434. https://doi.org/10.3390/cli3020416

Balsamo, G., Albergel, C., Beljaars, A., Boussetta, S., Brun, E., Cloke, H., et al. (2015). ERA-Interim/Land: A global land surface reanalysis data set. *Hydrology and Earth System Sciences*, *19*(1), 389–407. https://doi.org/10.5194/hess-19-389-2015

Balsamo, G., Beljaars, A., Scipal, K., Viterbo, P., van den Hurk, B., Hirschi, M., & Betts, A. K. (2009). A revised hydrology for the ECMWF model: Verification from field site to terrestrial water storage and impact in the integrated forecast system. *Journal of Hydrometeorology*, *10*(3), 623–643. https://doi.org/10.1175/2008jhm1068.1

Behera, S. K., Luo, J.-J., Masson, S., Delecluse, P., Gualdi, S., Navarra, A., & Yamagata, T. (2005). Paramount impact of the Indian Ocean Dipole on the East African short rains: A CGCM study. *Journal of Climate*, *18*(21), 4514–4530. https://doi.org/10.1175/jcli3541.1

Behera, S. K., & Yamagata, T. (2001). Subtropical SST dipole events in the southern Indian Ocean. *Geophysical Research Letters*, *28*(2), 327–330. https://doi.org/10.1029/2000GL011451

BfG. (2017). The Global Runoff Data Base (GRDB). Retrieved from: https://www.bafg.de/GRDC/EN/Home/homepage_node.html

Black, E. (2005). The relationship between Indian Ocean sea–surface temperature and East African rainfall. Philosophical Transactions of the Royal Society A: Mathematical. *Physical and Engineering Sciences*, *363*(1826), 43–47. https://doi.org/10.1098/rsta.2004.1474

Blamey, R. C., & Reason, C. J. C. (2013). The role of mesoscale convective complexes in southern Africa summer rainfall. *Journal of Climate*, *26*(5), 1654–1668. https://doi.org/10.1175/jcli-d-12-00239.1

Blöschl, G., Hall, J., Parajka, J., Perdigão, R. A. P., Merz, B., Arheimer, B., et al. (2017). Changing climate shifts timing of European floods. *Science*, *357*(6351), 588–590. https://doi.org/10.1126/science.aan2506

Burn, D. H. (1997). Catchment similarity for regional flood frequency analysis using seasonality measures. *Journal of Hydrology*, *202*(1-4), 212–230. https://doi.org/10.1016/S0022-1694(97)00068-1

Burn, D. H., Whitfield, P. H., & Sharif, M. (2016). Identification of changes in floods and flood regimes in Canada using a peaks over threshold approach. *Hydrological Processes*, *30*(18), 3303–3314. https://doi.org/10.1002/hyp.10861

Camberlin, P., Janicot, S., & Poccard, I. (2001). Seasonality and atmospheric dynamics of the teleconnection between African rainfall and tropical sea-surface temperature: Atlantic vs. ENSO. *International Journal of Climatology*, *21*(8), 973–1005. https://doi.org/10.1002/joc.673

Camberlin, P., Moron, V., Okoola, R., Philippon, N., & Gitau, W. (2009). Components of rainy seasons' variability in Equatorial East Africa: Onset, cessation, rainfall frequency and intensity. *Theoretical and Applied Climatology*, *98*(3-4), 237–249. https://doi.org/10.1007/s00704-009-0113-1

Chiew, F. H. S., & McMahon, T. A. (2002). Global ENSO-streamflow teleconnection, streamflow forecasting and interannual variability. *Hydrological Sciences Journal*, *47*(3), 505–522. https://doi.org/10.1080/02626660209492950

Coughlan de Perez, E., Stephens, E., Bischiniotis, K., van Aalst, M., van den Hurk, B., Mason, S., et al. (2017). Should seasonal rainfall forecasts be used for flood preparedness? *Hydrology and Earth System Sciences*, *21*(9), 4517–4524. https://doi.org/10.5194/hess-21-4517-2017

Cunderlik, J. M., & Ouarda, T. B. M. J. (2009). Trends in the timing and magnitude of floods in Canada. *Journal of Hydrology*, *375*(3-4), 471–480. https://doi.org/10.1016/j.jhydrol.2009.06.050

Dettinger, M. D., & Diaz, H. F. (2000). Global characteristics of stream flow seasonality and variability. *Journal of Hydrometeorology*, *1*(4), 289–310. https://doi.org/10.1175/1525-7541(2000)001<0289:GCOSFS>2.0.CO;2

Dunning, C. M., Black, E., & Allan, R. P. (2018). Later wet seasons with more intense rainfall over Africa under future climate change. *Journal of Climate*, *31*(23), 9719–9738. https://doi.org/10.1175/jcli-d-18-0102.1

Dunning, C. M., Black, E. C. L., & Allan, R. P. (2016). The onset and cessation of seasonal rainfall over Africa. *Journal of Geophysical Research: Atmospheres*, *121*, 11,405–11,424. https://doi.org/10.1002/2016JD025428

Emerton, R., Cloke, H. L., Stephens, E. M., Zsoter, E., Woolnough, S. J., & Pappenberger, F. (2017). Complex picture for likelihood of ENSO-driven flood hazard. *Nature Communications*, *8*(1), 14796. https://doi.org/10.1038/ncomms14796

FAO/GIEWS, F. (2018). GIEWS—Global Information and Early Warning System. Country Briefs. Retrieved from http://www.fao.org/giews/countrybrief/country.jsp?code=MOZ

Gelati, E., Madsen, H., & Rosbjerg, D. (2014). Reservoir operation using El Niño forecasts—Case study of Daule Peripa and Baba, Ecuador. *Hydrological Sciences Journal*, *59*(8), 1559–1581. https://doi.org/10.1080/02626667.2013.831978

Gu, G., & Adler, R. F. (2004). Seasonal evolution and variability associated with the West African monsoon system. *Journal of Climate*, *17*(17), 3364–3377. https://doi.org/10.1175/1520-0442(2004)017<3364:seavaw>2.0.co;2

Hachigonta, S., Reason, C. J. C., & Tadross, M. (2008). An analysis of onset date and rainy season duration over Zambia. *Theoretical and Applied Climatology*, *91*(1-4), 229–243. https://doi.org/10.1007/s00704-007-0306-4

Hastenrath, S. (1996). *Climate dynamics of the tropics*. Dordrecht: Kluwer Academic Publishers.

Herrmann, S. M., & Mohr, K. I. (2011). A continental-scale classification of rainfall seasonality regimes in Africa based on gridded precipitation and land surface temperature products. *Journal of Applied Meteorology and Climatology*, *50*(12), 2504–2513. https://doi.org/10.1175/JAMC-D-11-024.1

Hirpa, F. A., Salamon, P., Beck, H. E., Lorini, V., Alfieri, L., Zsoter, E., & Dadson, S. J. (2018). Calibration of the Global Flood Awareness System (GloFAS) using daily streamflow data. *Journal of Hydrology*, *566*, 595–606. https://doi.org/10.1016/j.jhydrol.2018.09.052

Huang, B., Thorne, P. W., Banzon, V. F., Boyer, T., Chepurin, G., Lawrimore, J. H., et al. (2017). Extended Reconstructed Sea Surface Temperature, version 5 (ERSSTv5): Upgrades, validations, and intercomparisons. *Journal of Climate*, *30*(20), 8179–8205. https://doi.org/10.1175/jcli-d-16-0836.1

Jammalamadaka, S. R., & SenGupta, A. (2001). In W. Scientific (Ed.), *Topics in circular statistics*. Singapore: World Scientific Press. https://doi.org/10.1142/4031

Kipkemboi, J. (2006). *Fingerponds: Seasonal integrated aquaculture in East African freshwater wetlands: Exploring their potential for wise use strategies* (PhD thesis, Wageningen University, Delft, The Netherlands). (Met lit. opg. - Met samenvatting in het Engels en Nederlands). Leiden, The Netherlands: Taylor & Francis. Retrieved from http://edepot.wur.nl/16528

Lee, D., Ward, P., & Block, P. (2015). Defining high-flow seasons using temporal streamflow patterns from a global model. *Hydrology and Earth System Sciences*, *19*(11), 4689–4705. https://doi.org/10.5194/hess-19-4689-2015

MacLeod, D. (2018). Seasonal predictability of onset and cessation of the east African rains. *Weather and Climate Extremes*, *21*, 27–35. https://doi.org/10.1016/j.wace.2018.05.003

Marchant, R., Mumbi, C., Behera, S., & Yamagata, T. (2007). The Indian Ocean dipole—The unsung driver of climatic variability in East Africa. *African Journal of Ecology*, *45*(1), 4–16. https://doi.org/10.1111/j.1365-2028.2006.00707.x

Mardia, K. V. (1972). In E. Birnbaum (Ed.), *Statistics of directional data*. New York, NY: Academic Press.

Mehari, A., Van Steenbergen, F., & Schultz, B. (2011). Modernization of spate irrigated agriculture: A new approach. *Irrigation and Drainage*, *60*(2), 163–173. https://doi.org/10.1002/ird.565

Moalafhi, D. B., Evans, J. P., & Sharma, A. (2016). Evaluating global reanalysis datasets for provision of boundary conditions in regional climate modelling. *Climate Dynamics*, *47*(9-10), 2727–2745. https://doi.org/10.1007/s00382-016-2994-x

Nash, D. J., & Endfield, G. H. (2008). "Splendid rains have fallen": links between El Niño and rainfall variability in the Kalahari, 1840–1900. *Climatic Change*, *86*(3-4), 257–290. https://doi.org/10.1007/s10584-007-9274-z

Nicholson, S. E. (2000). The nature of rainfall variability over Africa on time scales of decades to millenia. *Global and Planetary Change*, *26*(1-3), 137–158. https://doi.org/10.1016/S0921-8181(00)00040-0

Nicholson, S. E. (2017). Climate and climatic variability of rainfall over eastern Africa. *Reviews of Geophysics*, *55*, 590–635. https://doi.org/10.1002/2016RG000544

Nicholson, S. E., & Dezfuli, A. K. (2013). The relationship of rainfall variability in western equatorial Africa to the tropical oceans and atmospheric circulation. Part I: The Boreal Spring. *Journal of Climate*, *26*(1), 45–65. https://doi.org/10.1175/jcli-d-11-00653.1

Nicholson, S. E., & Entekhabi, D. (1987). Rainfall variability in equatorial and southern Africa: Relationships with sea surface temperatures along the southwestern coast of Africa. *Journal of Climate and Applied Meteorology*, *26*(5), 561–578. https://doi.org/10.1175/1520-0450(1987)026<0561:rvieas>2.0.co;2

Nicholson, S. E., & Kim, J. (1997). The relationship of the El Niño–Southern Oscillation to African rainfall. *International Journal of Climatology*, *17*(2), 117–135. https://doi.org/10.1002/(SICI)1097-0088(199702)17:2<117::AID-JOC84>3.0.CO;2-O

Oludhe, C., Sankarasubramanian, A., Sinha, T., Devineni, N., & Lall, U. (2013). The role of multimodel climate forecasts in improving water and energy management over the Tana River Basin, Kenya. *Journal of Applied Meteorology and Climatology*, *52*(11), 2460–2475. https://doi.org/10.1175/JAMC-D-12-0300.1

Paul, B. K. (1984). Perception of and agricultural adjustment to floods in Jamuna floodplain, Bangladesh. *Human Ecology*, *12*(1), 3–19. https://doi.org/10.1007/BF01531281

Phillips, J., & McIntyre, B. (2000). ENSO and interannual rainfall variability in Uganda: Implications for agricultural management. *International Journal of Climatology*, *20*(2), 171–182. https://doi.org/10.1002/(SICI)1097-0088(200002)20:2<171::AID-JOC471>3.0.CO;2-O

R Core Team, R. (2017). R: A language and environment for statistical computing. Vienna, Austria: R Foundation for Statistical Computing. Retrieved from https://www.R-project.org/

Reason, C. J. C., Hachigonta, S., & Phaladi, R. F. (2005). Interannual variability in rainy season characteristics over the Limpopo region of southern Africa. *International Journal of Climatology*, *25*(14), 1835–1853. https://doi.org/10.1002/joc.1228

Reason, C. J. C., & Smart, S. (2015). Tropical south east Atlantic warm events and associated rainfall anomalies over southern Africa. *Frontiers in Environmental Science*, *3*(24). https://doi.org/10.3389/fenvs.2015.00024

Rouault, M., Florenchie, P., Fauchereau, N., & Reason, C. J. C. (2003). South East tropical Atlantic warm events and southern African rainfall. *Geophysical Research Letters*, *30*(5), 8009. https://doi.org/10.1029/2002GL014840

Rowell, D. P. (2013). Simulating SST Teleconnections to Africa: What is the state of the art? *Journal of Climate*, *26*(15), 5397–5418. https://doi.org/10.1175/jcli-d-12-00761.1

Saji, N. H., Goswami, B. N., Vinayachandran, P. N., & Yamagata, T. (1999). A dipole mode in the tropical Indian Ocean. *Nature*, *401*(6751), 360–363. https://doi.org/10.1038/43854

Saji, N. H., & Yamagata, T. (2003). Possible impacts of Indian Ocean Dipole mode events on global climate. *Climate Research*, *25*(2), 151–169. https://doi.org/10.3354/cr025151

Scudder, T. (1991). The need and justification for maintaining transboundary flood regimes: The Africa case. *Natural Resources Journal*, *31*(1), 75–107.

Sharif, M., & Burn, D. (2009). Detection of linkages between extreme flow measures and climate indices. *International Journal of Civil, Environmental, Structural, Construction and Architectural Engineering*, *36*, 495–500.

Sharma, A., Wasko, C., & Lettenmaier, D. P. (2018). If precipitation extremes are increasing, why aren't floods? *Water Resources Research*, *54*, 8545–8551. https://doi.org/10.1029/2018WR023749

Singleton, A. T., & Reason, C. J. C. (2007). Variability in the characteristics of cut-off low pressure systems over subtropical southern Africa. *International Journal of Climatology*, *27*(3), 295–310. https://doi.org/10.1002/joc.1399

Spate Irrigation Network. (2015). Flood based farming systems in Africa. Retrieved from http://spate-irrigation.org/resource-documents/overview-papers/

van Steenbergen, F. (1997). Understanding the sociology of spate irrigation: cases from Balochistan. *Journal of Arid Environments*, *35*(2), 349–365. https://doi.org/10.1006/jare.1996.0171

Stephens, E., Day, J. J., Pappenberger, F., & Cloke, H. (2015). Precipitation and floodiness. *Geophysical Research Letters*, *42*, 10,316–310,323. https://doi.org/10.1002/2015GL066779

Stewart, I. T., Cayan, D. R., & Dettinger, M. D. (2005). Changes toward earlier streamflow timing across western North America. *Journal of Climate*, *18*(8), 1136–1155. https://doi.org/10.1175/jcli3321.1

Tadross, M. A., Hewitson, B. C., & Usman, M. T. (2005). The interannual variability of the onset of the maize growing season over South Africa and Zimbabwe. *Journal of Climate*, *18*(16), 3356–3372. https://doi.org/10.1175/jcli3423.1

Todd, M. C., & Washington, R. (2004). Climate variability in central equatorial Africa: Influence from the Atlantic sector. *Geophysical Research Letters*, *31*, L23202. https://doi.org/10.1029/2004GL020975

Van Der Knijff, J. M., Younis, J., & De Roo, A. P. J. (2010). LISFLOOD: A GIS-based distributed model for river basin scale water balance and flood simulation. *International Journal of Geographical Information Science*, *24*(2), 189–212. https://doi.org/10.1080/13658810802549154

Vitart, F., Anderson, D., & Stockdale, T. (2003). Seasonal forecasting of tropical cyclone landfall over Mozambique. *Journal of Climate*, *16*(23), 3932–3945. https://doi.org/10.1175/1520-0442(2003)016<3932:sfotcl>2.0.co;2

Ward, P. J., Jongman, B., Kummu, M., Dettinger, M. D., Sperna Weiland, F. C., & Winsemius, H. C. (2014). Strong influence of El Niño Southern Oscillation on flood risk around the world. *Proceedings of the National Academy of Sciences*, *111*(44), 15,659–15,664. https://doi.org/10.1073/pnas.1409822111

Wasko, C., & Sharma, A. (2017). Global assessment of flood and storm extremes with increased temperatures. *Scientific Reports*, *7*(1), 7945. https://doi.org/10.1038/s41598-017-08481-1

Wolff, C., Haug, G. H., Timmermann, A., Damste, J. S. S., Brauer, A., Sigman, D. M., et al. (2011). Reduced interannual rainfall variability in East Africa during the Last Ice Age. *Science*, *333*(6043), 743–747. https://doi.org/10.1126/science.1203724

Wolski, P., & Murray-Hudson, M. (2006). Flooding dynamics in a large low-gradient alluvial fan, the Okavango Delta, Botswana, from analysis and interpretation of a 30-year hydrometric record. *Hydrology and Earth System Sciences*, *10*(1), 127–137. https://doi.org/10.5194/hess-10-127-2006

Yang, W., Seager, R., Cane, M. A., & Lyon, B. (2015). The annual cycle of East African precipitation. *Journal of Climate*, *28*(6), 2385–2404. https://doi.org/10.1175/jcli-d-14-00484.1

Zajac, Z., Revilla-Romero, B., Salamon, P., Burek, P., Hirpa, F. A., & Beck, H. (2017). The impact of lake and reservoir parameterization on global streamflow simulation. *Journal of Hydrology*, *548*, 552–568. https://doi.org/10.1016/j.jhydrol.2017.03.022